HPV epitope processing differences correlate with ERAP1 allotype and extent of $CD8^+$ T cell tumor infiltration in OPSCC

Emma Reeves, Oliver Wood, Christian H. Ottensmeier, Emma V. King, Gareth J. Thomas, Tim Elliott, Edward James

Centre for Cancer Immunology, University of Southampton Faculty of Medicine, University Hospital Southampton, and Institute for Life sciences, University of Southampton, Southampton, UK

Running Title: ERAP1 trimming function in OPSCC

Keywords: ERAP1, OPSCC, HPV, antigen processing and presentation, $CD8^+$ T cells.

Correspondence:
Edd James
Centre for Cancer Immunology,
University Hospital Southampton,
Tremona Road,
Southampton SO16 6YD
Tel No. +44 2381205884
Fax No. +44 2381205152
Email: eddjames@soton.ac.uk

The authors declare no potential conflict of interests.

This work was supported by the Cancer Research UK Programme Grant A16997 awarded to E.J. and T.E.

Abstract

Presence of tumor infiltrating lymphocytes (TIL) predicts survival in many cancer types. In HPV-driven cancers, cervical and oropharyngeal squamous cell carcinomas (CSCC and OPSCC respectively), numbers of infiltrating T-cells, particularly $CD8^+$ T cells, and presentation of HPV E6/E7 epitopes are associated with improved prognosis. Endoplasmic reticulum aminopeptidase 1 (ERAP1) regulates the presented peptide repertoire, trimming peptide precursors prior to MHC I loading. ERAP1 is polymorphic, and allotypic variation of ERAP1 enzyme activity has an impact on the presented peptide repertoire. Individual single nucleotide polymorphisms are associated with incidence and outcome in a number of diseases, including CSCC. Here, we highlight the requirement for ERAP1 in the generation of HPV E6/E7 epitopes and show that the functional activity of ERAP1 allotype combinations identified in OPSCC correlate with tumor-infiltrating $CD8^+$ T cell (CD8)/TIL (CD8/TIL) status of the tumor. Functional analyses revealed that ERAP1 allotype combinations associated with CD8/TIL^{low} tumors have a reduced capacity to generate both a model antigen SIINFEHL and the HPV-16 $E7_{82\text{-}90}$ epitope LLMGTLGIV from N-terminally extended precursor peptides. In contrast, ERAP1 allotypes from CD8/TIL^{high} tumors generated the epitopes efficiently. These data reveal that ERAP1 function correlates with CD8/TIL numbers and, by implication, prognosis, suggesting that the presentation of HPV-16 epitopes at the cell surface, resulting in an anti-HPV T cell response, may depend on the ERAP1 allotype combinations expressed within an individual.

Introduction

Lymphocyte infiltration of tumors, in particular by $CD8^+$ T cells, is associated with better clinical outcome in many cancers (1-6). Although this tumor infiltration is driven by a number of factors such as expression of chemokines and their receptors, the presentation of immunogenic peptide epitopes is paramount. The identity of immunogenic peptide epitopes and hence, specificity of tumor infiltrating $CD8^+$ T cells, has not been determined in most instances, but it is likely that T cell specificity and efficacy are linked, as they are in other diseases. However, in human papillomavirus (HPV) driven cancers such as cervical squamous cell carcinoma (CSCC) and oropharyngeal squamous cell carcinoma (OPSCC), where HPV infection accounts for >95% and 40-80% of cases in the western world respectively, peripheral and tumor infiltrating $CD8^+$ T cells have been shown to recognize epitopes derived from the E6/E7 oncoproteins expressed by the virus (5, 7, 8). Furthermore, more tumor infiltrating $CD8^+$ T cells (TIL) in OPSCC is associated with improved survival (5, 9).

The presentation of peptide epitopes to $CD8^+$ T cells is dependent on the antigen processing pathway. Several components of this pathway are polymorphic, including HLA, endoplasmic reticulum aminopeptidase 1 (ERAP1), the transporter associated with antigen processing (TAP), and to a lesser extent Tapasin (10). ERAP1 trims N-terminally extended peptide epitopes to the correct length for optimal binding to HLA and therefore serves as an editor of the peptide repertoire presented at the cell surface. We have previously shown that ERAP1 allotypes arising from its polymorphism can differ in their peptide trimming function, defined by both overall activity and specificity for the N-terminal amino acid of peptide epitope precursors (11). In CSCC, genome wide association studies (GWAS) showed non-synonymous exonic single nucleotide polymorphisms (SNPs) of ERAP1 were associated with disease incidence (12), with two of these SNPs associated with disease-free and overall

survival (13). Given that CSCC is predominantly driven by HPV infection and, similar to OPSCC, shows improved survival with more TIL (14), the ability to control HPV^+ tumors is likely mediated by $CD8^+$ T cells specific for HPV-derived antigens (4, 5). Thus, the ability to generate and present peptide epitopes derived from viral proteins, such as E6 and E7, likely drives anti-tumor responses.

In this study, having observed similarities in SNP variants between CSCC and a cohort of HPV^+ OPSCC patients, we tested the hypothesis that allotypic variation in ERAP1 might underpin the extent of $CD8^+$ T cell tumor infiltration via its impact on processing of tumor-specific (HPV-derived) epitopes. In individual patients, we found that ERAP1 function correlates with tumor infiltrating $CD8^+$ T cell (CD8)/TIL (CD8/TIL) status in resected tumors: ERAP1 in $CD8/TIL^{low}$ tumors had reduced capacity to generate the HPV E7-derived epitope, LLMGTLGIV, suggesting that the lack of $CD8^+$ T cell infiltration may be linked to the ability to generate and present virally derived peptide epitopes. These data suggest that ERAP1 function may identify 'high-risk' OPSCC patients with poor prognosis.

Materials and Methods

Patients, HPV classification and CD8/TIL scoring

Patients previously classified for HPV^+ tumor status using HPV *in situ* hybridization (ISH) and p16 immunochemistry were used in this study (REC reference 09/H0501/90). Tumor histology was previously characterized for each patient (9) and reviewed for this study by pathologist GJT according to the 1998 UK Royal College of Pathologist Guidelines. Lymphocyte infiltrate (TIL) was determined and scored under low-power magnification (x2.5 objective) as high (diffuse; present in >80% of tumor/stroma), moderate (patchy; present in 20-80% of tumor/stroma) or low (weak/absent; present in <20% of tumor/stroma) (9). In addition, $CD8^+$ T cell infiltration was scored by immunohistochemistry and enumeration of $CD8^+$ T cells was expressed as an average of ten high-power fields (9). Images were collected using a CKX41 inverted microscope with DP-22 color camera running under CellSens (Version2) software and x10 or x40 achromat objective lenses (all Olympus, UK) (Supplementary Fig. S1A). Grouping was defined by the tertile values: high (>39 $CD8^+$ T cells/field), moderate (>13 and <39 $CD8^+$ T cells/field) and low (<13 $CD8^+$ T cells/field) (Supplementary Fig. S1B).

ERAP1 isolation and identification

ERAP1 was amplified from whole blood samples and cloned into the pcDNA3.1 expression vector (Life Technologies, UK) as described previously (11). ERAP1 clones from each patient were sequenced (Source Bioscience Ltd) and compared to the wild-type ERAP1 sequence (UniProt – Q9NZ08) to identify the presence of polymorphic variants using DNADynamo alignment software (Blue Tractor Software). To further validate the presence of ERAP1 polymorphisms, gDNA was extracted from whole blood using DNeasy Blood and

Tissue kit (Qiagen) and targeted ERAP1 exons amplified and sequenced using the following primers; M349V 5-GATGATTGTTTGGGAGAATG-3' and 5'-GCCTTATATGTCCACGCT-3', K528R 5'-CTTTCAGTCTGGTGCTATGG-3' and 5'-GTGTGATGGCTGGGGACATC-3', D575N 5'- GCTCTACTCAAGGAGTCCAAG-3' and 5'- CGATTTTCAATCTGATCCC-3' and R725Q/Q730E 5'-CCTGACTTTAAGTAGATGG-3' and 5'- GGTTATTTAGTAAGGACTGAC-3'.

DNA constructs

The pcDNA3.1 minigenes (ES)-SHL8, (ES)-X-SHL8, H2-K^{b}, ERAP1*002 as well as the non-functional active site ERAP1 mutant, E320A, have been described previously (11). The HPV-16 E7 epitope-specific construct (ES)-LV9 was generated by the insertion of oligonucleotides into the EcoRI/XbaI sites of pcDNA3.1, encoding the ER translocation signal sequence (ES) followed by the amino acid sequence LLMGTLGIV (LV9). The (ES)-X-LV9 constructs were generated by site directed mutagenesis to incorporate a single amino acid into the (ES)-LV9 construct, using the following primers: 5'-GCGGCAGTCTGCAGCGCG*NNS*CTGTTAATGGGCACACTAG-3' and 5'-CTAGTGTGCCCATTAACAG*SNN*CGCGCTGCAGACTGCCGC-3', where N = any nucleotide and S = C or G. Constructs were sequence verified, and the most frequent codon for each amino chosen for use where possible.

Dextramer detection of HPV-specific T cells

Patient tumor samples were mechanically disaggregated into single cell suspensions before being analyzed for the presence of HPV16-specific T cells by flow cytometry. Dextramers specific for HPV16 $E6_{18-26}$ (KLPQLCTEL; KL9), $E6_{29-38}$ (TIHDIILEV; TV10) and $E7_{82-90}$

(LLMGTLGIV; LV9) were obtained from Immudex and directly conjugated with PE, APC and FITC fluorophores, respectively. Tumor cells were pre-incubated with 50nM protein kinase inhibitor dasatanib for 30mins at 37^{o}C, before the addition of 10µl dextramer and incubated for a further 30mins at 4^{o}C. After two washes, surface antibodies for CD8 (anti-CD8-Pacific Blue, clone RPA-T8, BD Biosciences) and CD3 (anti-CD3-AmCyan, clone SK7, BD Biosciences) were incubated for 20mins at 4^{o}C before washing. Cells were acquired on BD FACS Canto II (BD Biosciences) and analyzed using Flow Jo Software (TreeStar Inc.).

Generation of BE7A2Z hybridoma

The generation of LacZ inducible T cell hybridomas has been described previously (15). Briefly, the BE7A2Z hybridoma was generated by immunizing HLA-A*0201 transgenic HHD mice with LLMGTLGIV-pulsed BMDC and splenocytes fused with the BWZ.36/CD8α cell line as described (15). To determine peptide specificity of the hybridoma, splenocytes were pulsed with 10µM LV9 or 10µM irrelevant peptide and hybridomas assessed for IFNγ production. To determine sensitivity of subsequent LV9-specific clones, 293T cells expressing endogenous HLA-A2, were pulsed with 10nM LV9 peptide and co-cultured with hybridoma clones for 24 hours. Each hybridoma clone sensitivity to LV9 was assessed by measurement of intracellular LacZ activity by chlorophenol red-β-d-galactopyranoside (CPRG; Roche).

Cell lines, transfection and T cell activation assay

Culture conditions for ERAP1 knockout HEK293T (293T E1KO) and T cell hybridoma cells have been described before (16). 293T E1KO cells were cultured from freshly thawed

aliquots from passage 2 (generated from original 293T cell line in 2013) and used over two weeks for the indicated experiments. Cells were authenticated by STR analysis and were confirmed mycoplasma free. For assessment of ERAP1 trimming activity, 293T E1KO cells were transfected with DNA using FuGENE 6 Transfection Reagent (Promega, UK). For assessment of single amino acid trimming specificity, 293T E1KO cells were transfected with 0.1μg total DNA, consisting of 0.05μg E320A non-functional ERAP1 or 0.025μg of each patient ERAP1 allotype, together with 0.025μg H2-K^b (SHL8) or HLA-A*0201 (LV9) and 0.025μg X-SHL8 or X-LV9. For assessment of LV9 extended precursor trimming (ED / D-LV9), 293T E1KO cells were transfected with 1μg total DNA, consisting of 0.5μg E320A or 0.25μg each patient ERAP1 allotype, together with 0.25μg ED/D-LV9 or LV9 and 0.25μg HLA-A*0201. All transfected cells were incubated for 24hours at 37^{o}C. Presentation of final peptide SHL8 or LV9 and activation of the respective LacZ-inducible T cell hybridoma, B3Z or BE7A2Z, was assessed by measurement of intracellular LacZ activity by CPRG.

Statistical analysis

Two or one-way ANOVA with Dunnett's post test was performed for analysis of differences between multiple groups and controls (GraphPad Prism).

Results

ERAP1 allotype sequences in OPSCC patients

ERAP1 polymorphism is associated with disease risk and disease-free survival in HPV induced CSCC (12, 13). For OPSCC, 40-80% of cases in the western world are also associated with HPV infection and within this group of patients, the amount of tumor infiltrating lymphocytes (TIL) observed in resected tumors correlates with disease survival (9, 17). We therefore investigated whether OPSCC patients shared the same ERAP1 polymorphisms observed in CSCC and whether the allotypes expressed in patients correlated with numbers of tumor infiltrating $CD8^+$ T cell (CD8)/TIL. We sequenced both ERAP1 copies expressed in a cohort of 26 OPSCC patients whose tumors had been scored with high, moderate or low numbers of CD8/TIL. Two of the CSCC-associated ERAP1 SNPs (P127 and E730) were detected in the majority of patients, regardless of CD8/TIL status, with E730 being more frequently observed (E730 = 9/10 $CD8/TIL^{high}$, 6/7 $CD8/TIL^{mod}$ and 7/8 $CD8/TIL^{low}$ patients; P127 = 8/10 $CD8/TIL^{high}$, 2/7 $CD8/TIL^{mod}$ and 4/8 $CD8/TIL^{low}$ patients; Table 1). The number of patients that contained both P127 and E730 varied between CD8/TIL groups with $CD8/TIL^{high}$ having the greatest proportion (8/10 versus 2/7 $CD8/TIL^{mod}$ and 4/8 $CD8/TIL^{low}$; Table 1). Examination of the two individual ERAP1 allotypes from each patient that contained either of the P127 or E730 variants in a single molecule ($CD8/TIL^{high}$ = 13/20 total allotypes; $CD8/TIL^{mod}$ = 11/14; $CD8/TIL^{low}$ = 12/16), revealed that a proportion did not contain both of the variants (P127 and E730) in the same molecule, with $CD8/TIL^{mod}$ and $CD8/TIL^{low}$ having the lowest frequency (8/13 TIL^{high}, 3/11 TIL^{mod}, 4/12 TIL^{low}; Table 1).

Overall, most of the allotypes observed have been previously described (*001; Hap10, *002; Hap2, *007, *011; Hap4, *013; Hap1, *014; Hap7, *015; Hap6, *018; Hap3 and *019; Hap5;

Table 1; (16, 18)). Two allotypes that have not previously been identified (*016, *017). Comparison of allotypes from different CD8/TIL groups showed that five allotypes were only found in one of the three groups, however, almost all of these represented a single incidence (Supplementary Table S1). Three allotypes were observed in all CD8/TIL groups and three in two groups (Supplementary Table S1), showing that, for this cohort, analysis of individual ERAP1 allotypes did not correlate with CD8/TIL status.

CD8/TIL^{low} allotype combinations have poor trimming function

We have previously shown, for an autoinflammatory disease, that the strongest association between ERAP1 and disease is achieved by considering ERAP1 allotype pairing, because this best represents the combined enzyme function of the co-dominantly expressed allotypes (16). We therefore investigated the peptide-editing function of ERAP1 allotype combinations in OPSCC patients utilizing the model system previously employed to assess trimming activity (11). This system classified ERAP1 allotypes with respect to their differential ability to generate a model epitope, SIINFEHL (SHL8) a modified form of SIINFEKL that stimulates T cells to the same degree as the original peptide (Supplementary Fig. S2), from precursor peptides with single amino acid N-terminal extensions in living cells. The SHL8/K^b complexes are detected at the cell surface by the specific T cell hybridoma, B3Z. Briefly, ERAP1 allotypes fall into three general classes of activity: those that process the epitope efficiently, those that are hypofunctional, and those that are hyperfunctional and overtrim the epitope, thus destroying it. Further differentiation of function is seen in N-terminal specificity. This assay is preferable to *in vitro* assays of function using small chromogenic substrates because it evaluates function *in vivo,* in the context of a functioning antigen

processing pathway, and provides a readout that relates directly to the impact on antigen presentation.

We analyzed the enzyme activity of ERAP1 allotype combinations that were observed exclusively in either high, moderate or low infiltrated tumors using this assay (Fig. 1A, B and C). Each allotype tested gave rise to a characteristic activity signature according to their relative ability to cleave X from the precursor substrate (where X is any one of the 20 naturally occurring amino acids). We also measured the activity of allotypes observed in both high and moderate infiltrated tumors (Fig. 1D), high and low infiltrated tumors (Fig. 1E) and in both moderate and low infiltrated tumors (Fig. 1F). The activity towards each substrate was expressed as a percentage of the maximal activity – observed with the SHL8 minigene (which does not require processing by ERAP1). By calculating the total activity across all substrates for each allotype combination as area under curve (AUC), we found that allotype combinations that were associated exclusively with low infiltrated tumors had a significantly reduced activity compared to those associated with high or moderate infiltrated tumors (50% and 55% respectively, Fig. 2A and B).

We next analyzed the specificity of each ERAP1 allotype combination by considering their activity against N-terminal extensions classified according to their physicochemical properties (aliphatic hydrophobic, aromatic hydrophobic, basic, acidic, uncharged polar). The results in Fig. 2C show that reduced activity of allotype combinations seen in CD8/TIL^{low} tumors is observed across all classes of N-terminal amino acid, closer inspection suggests that precursors with charged, polar uncharged or aliphatic hydrophobic N-1 amino acids are most effected (charged = 3/5 residues, polar uncharged = 3/4 residues, aliphatic = 2/4 residues were significantly reduced in CD8/TIL^{low} vs. CD8/TIL^{high}).

Anti-HPV CD8$^+$ T cell responses in OPSCC tumors

These observations are consistent with the hypothesis that the generation of epitopes requiring N-terminal trimming recruits CD8$^+$ T cells into the tumor mass and therefore that ERAP1 function is a determinant in this process. The data also suggest that the impact of ERAP1 polymorphism on CD8$^+$ T cell recruitment might be greatest for T cells recognizing epitopes generated from precursors with charged/polar uncharged/aliphatic hydrophobic amino acids. Better prognosis for HPV$^+$ OPSCC and CSCC patients is associated with more TIL (5, 9, 14) and there is evidence that CD8$^+$ T cells recognizing epitopes derived from the HPV E6/E7 proteins are among TIL in these cancers (5, 8, 19). We therefore scanned the immediate upstream sequence of predicted proteasomal cleavage products of E6 and E7 that contained a putative HLA-A*0201-restricted epitope (Table 2; (20-22)). Of the four E6 and four E7 derived peptides that have been confirmed as epitopes in previous studies (7, 23), three consisted of a core sequence with a predicted IC_{50} for HLA-A*0201 of less than 100nM. In addition, five of the eight peptides had a predicted one or two amino acid extension following proteasomal cleavage. However, only one of the epitopes had both an IC_{50} of less than 100nM and contained an N-terminal extension, HPV E7 82-90, LLMGTLGIV (LV9) (Table 2). The N-terminal extension of LV9 is comprised of acidic amino acids (Glu, Asp; ED-LV9) both of which were trimmed less efficiently by CD8/TIL^{low} allotype pairs when analyzed with the X-SHL8 substrate (Fig. 2C). In addition, the orthologue of this sequence from HPV-type 11 has been confirmed as an epitope in infected humans and so we selected LV9 for further analysis (24).

The precise immunodominance hierarchy of HLA-A*0201 restricted anti-HPV CD8$^+$ T cell responses has not been well characterized. To further confirm the role of LV9-CD8$^+$ T cells in anti-tumor immunity we assessed the presence of anti-HPV responses in five HPV$^+$ OPSCC tumors. Investigation of three E6/E7 peptide-specific responses, LV9, TV10 and

KL9, revealed that responses to all peptides were observed (Fig. 3A and B), with those directed to LV9 and TV10 the most prevalent. Indeed, LV9- and TV10-specific responses were dominant in two tumors (#1 and #4 versus #3 and #5 respectively), and co-dominant in one tumor (#2) (Fig. 3B). These responses confirmed LV9 as a good candidate peptide to investigate the role of ERAP1 in generation of HPV-derived antigenic peptides.

Cell surface presentation of LV9 epitope is ERAP1-dependent

To investigate the effect of ERAP1 on the generation of LV9 we created a T cell hybridoma recognizing LV9 restricted by HLA-A*0201 by immunizing HLA-A*0201 transgenic (HHD) mice with peptide-pulsed BMDC and fusing splenocytes harvested at day 7 after the final immunization with BWZ.36 CD8α^+ cells (15) (Supplementary Fig. S3A). Several hybridomas were generated and screened on LV9-pulsed splenocytes (Supplementary Fig. S3B). Four hybridomas were found to be peptide-specific and were stimulated by peptide pulsed HEK293T cells at the nanomolar quantities, with hybridoma #4 (called BE7A2Z) showing the greatest sensitivity and used in subsequent experiments (Supplementary Fig. S3C). To assess the *in vivo* processing of the LV9 peptide we transfected ERAP1 knockout HEK293T (E1KO 293T) cells with a minigene encoding the final (LV9) peptide. This construct sensitized both ERAP1-sufficient and E1KO 293T cells, whereas constructs encoding N-terminally extended LV9 (ED-LV9 and D-LV9) were generated only by ERAP1-sufficient cells, showing that *in vivo*, the processing of LV9 from these two precursor peptides is ERAP1 dependent (Supplementary Fig. S3D).

CD8/TIL^{low} allotype combinations have reduced functionality and different peptide specificity

We next measured the activity of ERAP1 allotype pairs that we identified exclusively in CD8/TIL high, moderate or low groups using X-LV9 minigene encoded substrates, as described above for X-SHL8. Examination of the allotype pairs showed a similar distribution of activities as for X-SHL8, with allotype pairs from CD8/TIL^{high} and CD8/TIL^{mod} patients having a significantly higher overall activity than those from CD8/TIL^{low} when the AUC was calculated (CD8/TIL^{high} = 45% and CD8/TIL^{mod} = 35% greater; Fig. 4A and B). Original data for the nine allotype combinations from CD8/TIL^{high}, ^{mod} and ^{low} groups are shown in Supplementary Fig. S4, A, B, and C respectively. Ala-, Cys-, Met-, Thr-, and Tyr-LV9 trimming by ERAP1 had a high background for E320A ERAP1, making it was difficult to confirm the amount of trimming of each allotype pair, consequently these data are not included. When we analyzed the specificity of N-terminus preference, we found significantly reduced responses for CD8/TIL^{low} compared to the other two CD8/TIL groups among the charged, polar uncharged and special N-terminal amino acid extensions (Fig. 4C). The trimming of Lys, Asp and Glu was more efficient in the context of the LV9 peptide backbone compared to SHL8 for all CD8/TIL groups (Lys = 15-50% for SHL8, 60-90% for LV9, Asp = 15-30% for SHL8, 50-70% for LV9 and Glu = 30-50% for SHL8, 85-90% for LV9; Figs. 2 and 4). Conversely, the aliphatic hydrophobic amino acids Ile and Leu were trimmed less efficiently in the context of LV9 than that observed for SHL8 (Ile = ~15-40% SHL8, 5-10% LV9 and Leu = 30-60% SHL8, 10-20% LV9; Figs. 2 and 4). These results indicate that although there are differences in amino acid specificity between substrates X-SHL8 and X-LV9, the total activity of CD8/TIL^{low} ERAP1 allotype pairs is reduced compared to that from CD8/TIL^{high} patients.

Generation of LV9 peptide epitope is impaired in CD8/TIL^{low} ERAP1 allotype pairs

The best prognosis for HPV^+ OPSCC is associated with high infiltration of $CD8^+$ T cells into the tumor (9), many of which are HPV-specific [Fig. 3; (5, 19, 25)]. With the reduced trimming capacity observed for CD8/TIL^{low} ERAP1 pairs, the ability to generate HPV-specific epitopes may be impaired preventing the activation and subsequent migration and infiltration of $CD8^+$ T cells into the tumor. To investigate the impact of ERAP1 on the generation of HPV-derived epitopes, we tested the ability of ERAP1 allotype combinations to generate the LV9 epitope from the minigene-encoded putative natural precursor (ED-LV9) across a range of effector:target ratios. Example results obtained from the allotype pair *001 + *002 found in CD8/TIL^{high} patients (#1, 4, 5, 10), *002 + *017 found in a CD8/TIL^{mod} patient (#13) and *007 + *011 from a CD8/TIL^{low} patient (#18) are shown in Fig. 5A. As a negative control, cells were transfected with the test precursor sequence together with an inactive mutant of *002 ERAP1 allotype (E320A). These experiments show a lower efficiency of CD8/TIL^{low}-associated allotype pairs in generating LV9 from both the single (D-) and double (ED-) N-terminal extended precursors compared to CD8/TIL^{high}, with ED-LV9 having the greatest reduction. When activity data from all allotype pairs observed were grouped according to the CD8/TIL status (Fig. 5B-E), it was evident that allotypes from CD8/TIL^{low} patients were less able to generate LV9 from either precursor, D-LV9 or ED-LV9, than allotypes from CD8/TIL^{high} and from ED-LV9 compared to CD8/TIL^{mod}. CD8/TIL^{high} pairs showed a 33% and 66% increase in the generation of LV9 from D-LV9 and ED-LV9 precursors respectively (Fig. 5B-E).

Examination of individual allotype pairs shows that the range of responses to both precursors observed for each CD8/TIL group overlap for both CD8/TIL^{high} and CD8/TIL^{mod}, but not CD8/TIL^{low} (D-LV9 = CD8/TIL^{high} 70-90%, CD8/TIL^{mod} 60-80% and CD8/TIL^{low} 50-60%; ED-LV9 = CD8/TIL^{high} 60-80%, CD8/TIL^{mod} 55-65% and TIL^{low} 40-45%; Fig. 4D and E). In particular, trimming of ED-LV9 showed stratification of allotype pairs based of CD8/TIL

numbers (Fig. 5E). The *007 allotype has been previously reported to be a hyperactive variant (16), therefore the reduced overall trimming activity in this CD8/TIL^{low} allotype pair is likely due to the dominant negative effect of allotype *007 (Fig. 5D and E). These results indicate that there is a correlation between CD8/TIL numbers and the ability to generate the HPV-E7 LV9 peptide epitope. Thus, the decreased cell surface expression of this HPV epitope in HPV-infected cells and tumors from CD8/TIL^{low} patients may compromise the ability of the immune system to recognize and kill HPV-infected cells.

Discussion

In this study, we investigated the correlation between ERAP1 allotype sequence and the amount of tumor infiltrating lymphocytes in 22 patients with HPV^+ OPSCC. $CD8^+$ T cell tumor infiltration has been linked with improved disease prognosis (5, 9). Examination of ERAP1 allotypes revealed that although many allotypes were shared between the CD8/TIL groups, some differentiation between patients with high versus low CD8/TIL numbers was seen even in this small sample. Moreover, we observed that ERAP1 allotype pairs expressed in the high CD8/TIL group had a greater trimming capacity compared to those identified from patients with low CD8/TIL numbers. This was further evident from the ability of the ERAP1 allotype pairs from different CD8/TIL groups to generate an E7 derived epitope, with low CD8/TIL ERAP1 pairs being poorer at generating the epitope and stimulating an LV9-specific T cell hybridoma. The anti-HPV T cell response in HPV^+ OPSCC patients, a cohort linked to a better response to therapy and prognosis (9, 26-29), is primarily directed towards antigens derived from the E6 and E7 oncoproteins (5, 7, 19). Indeed, we observed responses to three epitopes derived from these proteins in tumors. Thus, the reduced capacity to generate the E7 derived LV9 epitope by CD8/TIL low ERAP1 pairs suggests that ERAP1 activity may control presentation of epitopes derived from E6 and E7 that provoke anti-tumor T cell responses. In addition, within each CD8/TIL group, the ERAP1 pairs identified in patients had different peptide trimming specificities. This may explain why the correlation between ERAP1 identity and CD8/TIL level is not absolute.

ERAP1 polymorphism is associated with CSCC in GWAS (12). Despite the lack of GWAS of HPV^+ OPSCC, our observations of ERAP1 allotypes, both their sequence and functionality, are consistent with a common immunological mechanism between HPV^+ OPSCC and CSCC. SNPs in ERAP1 together with TAP2 and LMP7 (also part of the antigen processing pathway) are associated with a three-fold increase in cervical carcinoma risk (12).

In addition, downregulation of ERAP1 expression is an independent predictor of decreased overall survival and disease free survival in cervical carcinoma (30). In contrast, a study revealed ERAP1 expression was upregulated in head and neck squamous cell carcinoma (HNSCC) and HPV16$^+$ CSCC cell lines and cervical cancer (31). Although the identity of the overexpressed ERAP1 allotypes was not characterized in all cell lines in that study, to assess whether they expressed SNPs associated with CSCC risk, knockdown of ERAP1 in one of two cervical cancer cell lines in which ERAP1 alleles were identified resulted in increased killing by $E7_{81-91}$-specific T cells. This cell line expressed ERAP1 that is known to efficiently trim peptides, but for this epitope overtrims instead, indicating that ERAP1 can affect the presentation of HPV-derived epitopes. Therefore, the differences in function we have observed between ERAP1 allotypes could be relevant for controlling HPV associated cancer. We did not examine expression of the different ERAP1 allotypes in tumors in this study, but altering expression of specific ERAP1 allotypes that are efficient trimmers, such as *002, when co-expressed with a poor trimmer, *001, within the tumor may alter the ability to generate of tumor epitopes and diminish CD8$^+$ T cell activation. How the identity and expression of different ERAP1 allotype pairs affect generation of HPV-derived E6/E7 epitopes and their correlation with the antigen-specificity of HPV-specific CD8$^+$ T cells in patient cohorts, and whether these correlate with positive outcome and response to checkpoint blockade therapy, remains unclear. ERAP1 allotypes expressed in germline DNA may provide a biomarker for prognosis that would guide the patient's care pathway at the time of diagnosis.

The mechanism by which ERAP1 trims peptides and the factors that determine the efficacy of trimming such as the backbone sequence and the amino acid preceding the peptide (N-1) is poorly understood. Assessment of the trimming efficacy of ERAP1 containing single SNP variants showed that the catalytic rate of the variant enzymes was affected to a similar degree

for a number of peptide substrates with different backbones (32). The identity of the N-1 amino acid, however, influenced the ability of ERAP1 to generate the final peptide epitope (11, 33) suggesting that the N-1 amino acid affects trimming to a greater extent than the backbone. Consistent with this, we found that for two different peptide backbones, SHL8 and LV9 (which bind to different MHC molecules), the general trimming activity of the different ERAP1 pairs was similar. However, we found that the precise amino acid trimming specificity profiles of ERAP1 allotypes/pairs were different between X-SHL8 and X-LV9. For example, the 'top' three specificities for the single allotype *015 (CD8/TIL^{mod}), were E, H and Q for X-SHL8, and E, H and K for X-LV9. For single allotype *001 (CD8/TIL^{low}) we observed a greater difference where the 'top' three specificities were C, A and E for X-SHL8, but E, K and N for X-LV9. These differences indicate that compared to overall trimming phenotype, amino acid specificity profiles may depend on the peptide backbone. A greater understanding of how these specificity profiles relate to the core peptide sequence could enable the development of ERAP1 processing algorithms for individual and combined allotypes. This could be integrated with algorithms that predict proteasome cleavage (20-22), peptide binding affinity (34), and the effects of peptide abundance and intracellular competition (35) to improve the ability to predict whether candidate peptides are likely to be presented at the cell surface in sufficient abundance to prime an effective CTL response.

ERAP2, a homolog of ERAP1 that is less polymorphic, may also play a role in the generation of HPV-derived epitopes. ERAP2 has altered substrate handling and amino acid trimming preferences compared to ERAP1, showing a preference for Arg (R) and less enzymatic activity (36). Despite its reduced activity, ERAP2 likely also contributes to the generation of HPV-derived epitopes.

Currently three commercially available prophylactic HPV vaccines target high risk HPV-types (37). These vary in efficacy for prevention of both CIN2^{+} and CIN3^{+} (37). Neither of

these vaccines are effective at eliminating pre-existing HPV infections (38, 39) and therefore, infected individuals remain at risk. The clearance of established HPV infections is associated with $CD4^+$ T-helper 1 and $CD8^+$ T cells (40), with the E6 and E7 oncoproteins targets for the response. No therapeutic vaccines are yet available despite several promising clinical trials (41-43). One contributing factor to this failure may be related to ERAP1, as the expression of particular ERAP1 allotype pairs may prevent or reduce the capacity to generate immunogenic E6/E7 peptide epitopes. Thus, affecting the ability of antigen presenting cells to prime HPV-specific $CD8^+$ T cell responses in tumor draining LN and, for T cells that traffic to the tumor, the ability of tumor cells to activate them. Future vaccine design may need to incorporate the effect different ERAP1 allotypes have on the generation of candidate HPV-derived epitopes. In addition, the use of ERAP1 inhibitors (44, 45) alone or in combination with vaccines may prevent destruction of immunogenic epitopes through overtrimming by ERAP1 allotypes (46, 47) enabling activation of anti-HPV $CD8^+$ T cell responses and tumor protection.

In conclusion, this study demonstrates that the function of expressed ERAP1 allotypes correlates with the amount of infiltrating lymphocytes in tumors of OPSCC patients and thus, prognosis. $CD8/TIL^{low}$ ERAP1 allotype pairs were poor at generating an HPV E7 epitope indicating that the lack of T cell infiltration and subsequent poorer anti-tumor response may be related to the ability of HPV-infected/tumor cells to generate HPV-specific peptide epitopes.

Acknowledgements

The authors would like to thank Pandurangan Vijayanand for his support in collating samples and Nasia Kontouli for technical support. This work was supported by Cancer Research UK Programme Grant A16997 awarded to E.J. and T.E.

References:

1. Galon, J., A. Costes, F. Sanchez-Cabo, A. Kirilovsky, B. Mlecnik, C. Lagorce-Pages, M. Tosolini, M. Camus, A. Berger, P. Wind, F. Zinzindohoue, P. Bruneval, P. H. Cugnenc, Z. Trajanoski, W. H. Fridman, and F. Pages. 2006. Type, density, and location of immune cells within human colorectal tumors predict clinical outcome. *Science* 313: 1960-1964.
2. Leffers, N., M. J. Gooden, R. A. de Jong, B. N. Hoogeboom, K. A. ten Hoor, H. Hollema, H. M. Boezen, A. G. van der Zee, T. Daemen, and H. W. Nijman. 2009. Prognostic significance of tumor-infiltrating T-lymphocytes in primary and metastatic lesions of advanced stage ovarian cancer. *Cancer Immunol Immunother* 58: 449-459.
3. Noble, F., T. Mellows, L. H. McCormick Matthews, A. C. Bateman, S. Harris, T. J. Underwood, J. P. Byrne, I. S. Bailey, D. M. Sharland, J. J. Kelly, J. N. Primrose, S. S. Sahota, A. R. Bateman, G. J. Thomas, and C. H. Ottensmeier. 2016. Tumor infiltrating lymphocytes correlate with improved survival in patients with oesophageal adenocarcinoma. *Cancer Immunol Immunother* 65: 651-662.
4. Piersma, S. J., E. S. Jordanova, M. I. van Poelgeest, K. M. Kwappenberg, J. M. van der Hulst, J. W. Drijfhout, C. J. Melief, G. G. Kenter, G. J. Fleuren, R. Offringa, and S. H. van der Burg. 2007. High number of intraepithelial $CD8^+$ tumor-infiltrating lymphocytes is associated with the absence of lymph node metastases in patients with large early-stage cervical cancer. *Cancer Res* 67: 354-361.
5. Welters, M. J. P., W. Ma, S. Santegoets, R. Goedemans, I. Ehsan, E. S. Jordanova, V. J. van Ham, V. van Unen, F. Koning, S. I. van Egmond, P. Charoentong, Z. Trajanoski, L. A. van der Velden, and S. H. van der Burg. 2018. Intratumoral HPV16-Specific T Cells Constitute a Type I-Oriented Tumor Microenvironment to Improve Survival in HPV16-Driven Oropharyngeal Cancer. *Clin Cancer Res* 24: 634-647.
6. Brambilla, E., G. Le Teuff, S. Marguet, S. Lantuejoul, A. Dunant, S. Graziano, R. Pirker, J. Y. Douillard, T. Le Chevalier, M. Filipits, R. Rosell, R. Kratzke, H. Popper, J. C. Soria, F. A. Shepherd, L. Seymour, and M. S. Tsao. 2016. Prognostic Effect of Tumor Lymphocytic Infiltration in Resectable Non-Small-Cell Lung Cancer. *J Clin Oncol* 34: 1223-1230.
7. Albers, A., K. Abe, J. Hunt, J. Wang, A. Lopez-Albaitero, C. Schaefer, W. Gooding, T. L. Whiteside, S. Ferrone, A. DeLeo, and R. L. Ferris. 2005. Antitumor activity of human papillomavirus type 16 E7-specific T cells against virally infected squamous cell carcinoma of the head and neck. *Cancer Res* 65: 11146-11155.
8. de Vos van Steenwijk, P. J., M. Heusinkveld, T. H. Ramwadhdoebe, M. J. Lowik, J. M. van der Hulst, R. Goedemans, S. J. Piersma, G. G. Kenter, and S. H. van der Burg. 2010. An unexpectedly large polyclonal repertoire of HPV-specific T cells is poised for action in patients with cervical cancer. *Cancer Res* 70: 2707-2717.
9. Ward, M. J., S. M. Thirdborough, T. Mellows, C. Riley, S. Harris, K. Suchak, A. Webb, C. Hampton, N. N. Patel, C. J. Randall, H. J. Cox, S. Jogai, J. Primrose, K. Piper, C. H. Ottensmeier, E. V. King, and G. J. Thomas. 2014. Tumor-infiltrating lymphocytes predict for outcome in HPV-positive oropharyngeal cancer. *Br J Cancer* 110: 489-500.
10. Blum, J. S., P. A. Wearsch, and P. Cresswell. 2013. Pathways of antigen processing. *Annu Rev Immunol* 31: 443-473.
11. Reeves, E., C. J. Edwards, T. Elliott, and E. James. 2013. Naturally occurring ERAP1 haplotypes encode functionally distinct alleles with fine substrate specificity. *J Immunol* 191: 35-43.

12. Mehta, A. M., E. S. Jordanova, T. van Wezel, H. W. Uh, W. E. Corver, K. M. Kwappenberg, W. Verduijn, G. G. Kenter, S. H. van der Burg, and G. J. Fleuren. 2007. Genetic variation of antigen processing machinery components and association with cervical carcinoma. *Genes Chromosomes Cancer* 46: 577-586.
13. Mehta, A. M., E. S. Jordanova, W. E. Corver, T. van Wezel, H. W. Uh, G. G. Kenter, and G. Jan Fleuren. 2009. Single nucleotide polymorphisms in antigen processing machinery component ERAP1 significantly associate with clinical outcome in cervical carcinoma. *Genes Chromosomes Cancer* 48: 410-418.
14. Komdeur, F. L., T. M. Prins, S. van de Wall, A. Plat, G. B. A. Wisman, H. Hollema, T. Daemen, D. N. Church, M. de Bruyn, and H. W. Nijman. 2017. CD103+ tumor-infiltrating lymphocytes are tumor-reactive intraepithelial $CD8^+$ T cells associated with prognostic benefit and therapy response in cervical cancer. *Oncoimmunology* 6: e1338230.
15. Sanderson, S., and N. Shastri. 1994. LacZ inducible, antigen/MHC-specific T cell hybrids. *Int Immunol* 6: 369-376.
16. Reeves, E., A. Colebatch-Bourn, T. Elliott, C. J. Edwards, and E. James. 2014. Functionally distinct ERAP1 allotype combinations distinguish individuals with Ankylosing Spondylitis. *Proc Natl Acad Sci U S A* 111: 17594-17599.
17. Wansom, D., E. Light, F. Worden, M. Prince, S. Urba, D. B. Chepeha, K. Cordell, A. Eisbruch, J. Taylor, N. D'Silva, J. Moyer, C. R. Bradford, D. Kurnit, B. Kumar, T. E. Carey, and G. T. Wolf. 2010. Correlation of cellular immunity with human papillomavirus 16 status and outcome in patients with advanced oropharyngeal cancer. *Arch Otolaryngol Head Neck Surg* 136: 1267-1273.
18. Ombrello, M. J., D. L. Kastner, and E. F. Remmers. 2015. Endoplasmic reticulum-associated amino-peptidase 1 and rheumatic disease: genetics. *Curr Opin Rheumatol* 27: 349-356.
19. Heusinkveld, M., R. Goedemans, R. J. Briet, H. Gelderblom, J. W. Nortier, A. Gorter, V. T. Smit, A. P. Langeveld, J. C. Jansen, and S. H. van der Burg. 2012. Systemic and local human papillomavirus 16-specific T-cell immunity in patients with head and neck cancer. *Int J Cancer* 131: E74-85.
20. Hakenberg, J., A. K. Nussbaum, H. Schild, H. G. Rammensee, C. Kuttler, H. G. Holzhutter, P. M. Kloetzel, S. H. Kaufmann, and H. J. Mollenkopf. 2003. MAPPP: MHC class I antigenic peptide processing prediction. *Appl Bioinformatics* 2: 155-158.
21. Kuttler, C., A. K. Nussbaum, T. P. Dick, H. G. Rammensee, H. Schild, and K. P. Hadeler. 2000. An algorithm for the prediction of proteasomal cleavages. *J Mol Biol* 298: 417-429.
22. Nielsen, M., C. Lundegaard, O. Lund, and C. Kesmir. 2005. The role of the proteasome in generating cytotoxic T-cell epitopes: insights obtained from improved predictions of proteasomal cleavage. *Immunogenetics* 57: 33-41.
23. Ressing, M. E., A. Sette, R. M. Brandt, J. Ruppert, P. A. Wentworth, M. Hartman, C. Oseroff, H. M. Grey, C. J. Melief, and W. M. Kast. 1995. Human CTL epitopes encoded by human papillomavirus type 16 E6 and E7 identified through in vivo and in vitro immunogenicity studies of HLA-A*0201-binding peptides. *J Immunol* 154: 5934-5943.
24. Xu, Y., K. J. Zhu, X. Z. Chen, K. J. Zhao, Z. M. Lu, and H. Cheng. 2008. Mapping of cytotoxic T lymphocytes epitopes in E7 antigen of human papillomavirus type 11. *Arch Dermatol Res* 300: 235-242.
25. Krishna, S., P. Ulrich, E. Wilson, F. Parikh, P. Narang, S. Yang, A. K. Read, S. Kim-Schulze, J. G. Park, M. Posner, M. A. Wilson Sayres, A. Sikora, and K. S. Anderson.

2018. Human Papilloma Virus Specific Immunogenicity and Dysfunction of CD8(+) T Cells in Head and Neck Cancer. *Cancer Res* 78: 6159-6170.

26. Badoual, C., S. Hans, N. Merillon, C. Van Ryswick, P. Ravel, N. Benhamouda, E. Levionnois, M. Nizard, A. Si-Mohamed, N. Besnier, A. Gey, R. Rotem-Yehudar, H. Pere, T. Tran, C. L. Guerin, A. Chauvat, E. Dransart, C. Alanio, S. Albert, B. Barry, F. Sandoval, F. Quintin-Colonna, P. Bruneval, W. H. Fridman, F. M. Lemoine, S. Oudard, L. Johannes, D. Olive, D. Brasnu, and E. Tartour. 2013. PD-1-expressing tumor-infiltrating T cells are a favorable prognostic biomarker in HPV-associated head and neck cancer. *Cancer Res* 73: 128-138.
27. Oguejiofor, K., H. Galletta-Williams, S. J. Dovedi, D. L. Roberts, P. L. Stern, and C. M. West. 2017. Distinct patterns of infiltrating $CD8^+$ T cells in HPV^+ and CD68 macrophages in HPV- oropharyngeal squamous cell carcinomas are associated with better clinical outcome but PD-L1 expression is not prognostic. *Oncotarget* 8: 14416-14427.
28. Ang, K. K., J. Harris, R. Wheeler, R. Weber, D. I. Rosenthal, P. F. Nguyen-Tan, W. H. Westra, C. H. Chung, R. C. Jordan, C. Lu, H. Kim, R. Axelrod, C. C. Silverman, K. P. Redmond, and M. L. Gillison. 2010. Human papillomavirus and survival of patients with oropharyngeal cancer. *N Engl J Med* 363: 24-35.
29. Fakhry, C., W. H. Westra, S. Li, A. Cmelak, J. A. Ridge, H. Pinto, A. Forastiere, and M. L. Gillison. 2008. Improved survival of patients with human papillomavirus-positive head and neck squamous cell carcinoma in a prospective clinical trial. *J Natl Cancer Inst* 100: 261-269.
30. Mehta, A. M., E. S. Jordanova, G. G. Kenter, S. Ferrone, and G. J. Fleuren. 2008. Association of antigen processing machinery and HLA class I defects with clinicopathological outcome in cervical carcinoma. *Cancer Immunol Immunother* 57: 197-206.
31. Steinbach, A., J. Winter, M. Reuschenbach, R. Blatnik, A. Klevenz, M. Bertrand, S. Hoppe, M. von Knebel Doeberitz, A. K. Grabowska, and A. B. Riemer. 2017. ERAP1 overexpression in HPV-induced malignancies: A possible novel immune evasion mechanism. *Oncoimmunology* 6: e1336594.
32. Evnouchidou, I., R. P. Kamal, S. S. Seregin, Y. Goto, M. Tsujimoto, A. Hattori, P. V. Voulgari, A. A. Drosos, A. Amalfitano, I. A. York, and E. Stratikos. 2011. Cutting Edge: Coding single nucleotide polymorphisms of endoplasmic reticulum aminopeptidase 1 can affect antigenic peptide generation in vitro by influencing basic enzymatic properties of the enzyme. *J Immunol* 186: 1909-1913.
33. Hearn, A., I. A. York, and K. L. Rock. 2009. The specificity of trimming of MHC class I-presented peptides in the endoplasmic reticulum. *J Immunol* 183: 5526-5536.
34. Andreatta, M., and M. Nielsen. 2016. Gapped sequence alignment using artificial neural networks: application to the MHC class I system. *Bioinformatics* 32: 511-517.
35. Boulanger, D. S. M., R. C. Eccleston, A. Phillips, P. V. Coveney, T. Elliott, and N. Dalchau. 2018. A Mechanistic Model for Predicting Cell Surface Presentation of Competing Peptides by MHC Class I Molecules. *Frontiers in Immunology* 9.
36. Evnouchidou, I., J. Birtley, S. Seregin, A. Papakyriakou, E. Zervoudi, M. Samiotaki, G. Panayotou, P. Giastas, O. Petrakis, D. Georgiadis, A. Amalfitano, E. Saridakis, I. M. Mavridis, and E. Stratikos. 2012. A common single nucleotide polymorphism in endoplasmic reticulum aminopeptidase 2 induces a specificity switch that leads to altered antigen processing. *J Immunol* 189: 2383-2392.
37. Harper, D. M., and L. R. DeMars. 2017. HPV vaccines - A review of the first decade. *Gynecol Oncol* 146: 196-204.

38. Olsson, S. E., S. K. Kjaer, K. Sigurdsson, O. E. Iversen, M. Hernandez-Avila, C. M. Wheeler, G. Perez, D. R. Brown, L. A. Koutsky, E. H. Tay, P. Garcia, K. A. Ault, S. M. Garland, S. Leodolter, G. W. Tang, D. G. Ferris, J. Paavonen, M. Lehtinen, M. Steben, F. X. Bosch, J. Dillner, E. A. Joura, S. Majewski, N. Munoz, E. R. Myers, L. L. Villa, F. J. Taddeo, C. Roberts, A. Tadesse, J. Bryan, R. Maansson, S. Vuocolo, T. M. Hesley, A. Saah, E. Barr, and R. M. Haupt. 2009. Evaluation of quadrivalent HPV 6/11/16/18 vaccine efficacy against cervical and anogenital disease in subjects with serological evidence of prior vaccine type HPV infection. *Hum Vaccin* 5: 696-704.
39. Paavonen, J., P. Naud, J. Salmeron, C. M. Wheeler, S. N. Chow, D. Apter, H. Kitchener, X. Castellsague, J. C. Teixeira, S. R. Skinner, J. Hedrick, U. Jaisamrarn, G. Limson, S. Garland, A. Szarewski, B. Romanowski, F. Y. Aoki, T. F. Schwarz, W. A. Poppe, F. X. Bosch, D. Jenkins, K. Hardt, T. Zahaf, D. Descamps, F. Struyf, M. Lehtinen, G. Dubin, and H. P. S. Group. 2009. Efficacy of human papillomavirus (HPV)-16/18 AS04-adjuvanted vaccine against cervical infection and precancer caused by oncogenic HPV types (PATRICIA): final analysis of a double-blind, randomised study in young women. *Lancet* 374: 301-314.
40. van der Burg, S. H., and C. J. Melief. 2011. Therapeutic vaccination against human papilloma virus induced malignancies. *Curr Opin Immunol* 23: 252-257.
41. Kim, H. J., and H. J. Kim. 2017. Current status and future prospects for human papillomavirus vaccines. *Arch Pharm Res* 40: 1050-1063.
42. Vici, P., L. Pizzuti, L. Mariani, G. Zampa, D. Santini, L. Di Lauro, T. Gamucci, C. Natoli, P. Marchetti, M. Barba, M. Maugeri-Sacca, D. Sergi, F. Tomao, E. Vizza, S. Di Filippo, F. Paolini, G. Curzio, G. Corrado, A. Michelotti, G. Sanguineti, A. Giordano, R. De Maria, and A. Venuti. 2016. Targeting immune response with therapeutic vaccines in premalignant lesions and cervical cancer: hope or reality from clinical studies. *Expert Rev Vaccines* 15: 1327-1336.
43. Yang, A., E. Farmer, T. C. Wu, and C. F. Hung. 2016. Perspectives for therapeutic HPV vaccine development. *J Biomed Sci* 23: 75.
44. Weglarz-Tomczak, E., S. Vassiliou, and A. Mucha. 2016. Discovery of potent and selective inhibitors of human aminopeptidases ERAP1 and ERAP2 by screening libraries of phosphorus-containing amino acid and dipeptide analogues. *Bioorg Med Chem Lett* 26: 4122-4126.
45. Zervoudi, E., E. Saridakis, J. R. Birtley, S. S. Seregin, E. Reeves, P. Kokkala, Y. A. Aldhamen, A. Amalfitano, I. M. Mavridis, E. James, D. Georgiadis, and E. Stratikos. 2013. Rationally designed inhibitor targeting antigen-trimming aminopeptidases enhances antigen presentation and cytotoxic T-cell responses. *Proc Natl Acad Sci U S A* 110: 19890-19895.
46. James, E., I. Bailey, G. Sugiyarto, and T. Elliott. 2013. Induction of protective antitumor immunity through attenuation of ERAAP function. *J Immunol* 190: 5839-5846.
47. Keller, M., F. Ebstein, E. Burger, K. Textoris-Taube, X. Gorny, S. Urban, F. Zhao, T. Dannenberg, A. Sucker, C. Keller, L. Saveanu, E. Kruger, H. J. Rothkotter, B. Dahlmann, P. Henklein, A. Voigt, U. Kuckelkorn, A. Paschen, P. M. Kloetzel, and U. Seifert. 2015. The proteasome immunosubunits, PA28 and ER-aminopeptidase 1 protect melanoma cells from efficient MART-126-35 -specific T-cell recognition. *Eur J Immunol* 45: 3257-3268.

Table 1: ERAP1 allotype identity in OPSCC patients. Bold type indicates variants at the indicated amino acid position

Patient number	CD8/TIL status	ERAP1 allotype	Amino acid at indicated position							
			56	127	346	349	528	575	725	730
			E	**R**	**G**	**M**	**K**	**D**	**R**	**Q**
1	High	*001	E	**P**	G	**V**	**R**	**N**	**Q**	**E**
		*002	E	R	G	M	K	D	R	Q
2	“	*011	E	R	G	M	**R**	D	R	**E**
		*016	E	R	G	**V**	K	D	**Q**	**E**
3	“	*001	E	**P**	G	**V**	**R**	**N**	**Q**	**E**
		*018	E	R	G	M	K	D	R	**E**
4	“	*001	E	**P**	G	**V**	**R**	**N**	**Q**	**E**
		*002	E	R	G	M	K	D	R	Q
5	“	*001	E	**P**	G	**V**	**R**	**N**	**Q**	**E**
		*002	E	R	G	M	K	D	R	Q
6	“	*002	E	R	G	M	K	D	R	Q
		*002	E	R	G	M	K	D	R	Q
7	“	*002	E	R	G	M	K	D	R	Q
		*014	**K**	**P**	G	M	**R**	D	R	**E**
8	“	*001	E	**P**	G	**V**	**R**	**N**	**Q**	**E**
		*011	E	R	G	M	**R**	D	R	**E**
9	“	*011	E	R	G	M	**R**	D	R	**E**
		*015	E	**P**	G	M	**R**	D	R	**E**
10	“	*001	E	**P**	G	**V**	**R**	**N**	**Q**	**E**
		*002	E	R	G	M	K	D	R	Q
11	Moderate	*015	E	**P**	G	M	**R**	D	R	**E**
		*015	E	**P**	G	M	**R**	D	R	**E**
12	“	*001	E	**P**	G	**V**	**R**	**N**	**Q**	**E**
		*011	E	R	G	M	**R**	D	R	**E**
13	“	*002	E	R	G	M	K	D	R	Q
		*017	E	R	G	M	K	**N**	R	Q
14	“	*011	E	R	G	M	**R**	D	R	**E**
		*018	E	R	G	M	K	D	R	**E**
15	“	*002	E	R	G	M	K	D	R	Q
		*011	E	R	G	M	**R**	D	R	**E**
16	“	*011	E	R	G	M	**R**	D	R	**E**
		*011	E	R	G	M	**R**	D	R	**E**
17	“	*016	E	R	G	**V**	K	D	**Q**	**E**
		*018	E	R	G	M	K	D	R	**E**
18	Low	*007	E	R	G	M	**R**	D	**Q**	Q
		*011	E	R	G	M	**R**	D	R	**E**
19	“	*001	E	**P**	G	**V**	**R**	**N**	**Q**	**E**
		*019	E	R	**D**	M	**R**	D	R	**E**
20	“	*001	E	**P**	G	**V**	**R**	**N**	**Q**	**E**
		*001	E	**P**	G	**V**	**R**	**N**	**Q**	**E**
21	“	*011	E	R	G	M	**R**	D	R	**E**
		*011	E	R	G	M	**R**	D	R	**E**
22	“	*013	E	**P**	G	M	K	D	R	Q
		*019	E	R	**D**	M	**R**	D	R	**E**
23	“	*002	E	R	G	M	K	D	R	Q
		*002	E	R	G	M	K	D	R	Q
24	“	*002	E	R	G	M	K	D	R	Q

		*011	E	R	G	M	**R**	D	R	**E**
25	“	*011	E	R	G	M	**R**	D	R	**E**
		*011	E	**P**	G	M	**R**	D	R	**E**

Table 2: HLA-A*0201 restricted HPV-16 E6/E7 peptide epitopes

Protein	Position (amino acid)	Epitope sequence	MHC IC_{50} (predicted nM) NetMHC	Predicted proteasome cleaved peptide (N-terminal extension) NetCHOP, MAPPP
E6	7-15	AMFQDPQER	-	**RT**AMFQDPQER
E6	18-26	KLPQLCTEL	134.4	**PR**KLPQLCTEL
E6	29-38	TIHDIILECV	200.6	**QT**TIHDIILECV/TIHDIILECV
E6	42-50	FAFRDLCIV	100.4	**D**FAFRDLCIV
E7	7-15	TLHEYMLDL	94.1	TLHEYMLDL
E7	11-19(20)	YMLDLQPET(T)	10.58 (33.3)	YMLDLQPET(T)
E7	82-90	LLMGTLGIV	37.11	**ED**LLMGTLGIV/**D**LLMGTLGIV
E7	86-93	TLGIVCPI	409.85	TLGIVCPI

Figure Legends

Figure 1. N-terminal amino acid trimming specificity by OPSCC ERAP1 allotype combinations.

E1KO 293T cells were transfected with ERAP1 allotype combinations from OPSCC patients together with H2-K^b and X-SHL8 minigenes representing 20 amino acids and assessed for generation of SHL8 by B3Z activation. OPSCC ERAP1 allotype identity from patients with TIL status are shown in panels (A) CD8/TIL^{high}, (B) CD8/$TIL^{moderate}$, (C) CD8/TIL^{Low}, (D) CD8/TIL^{high} and CD8/$TIL^{moderate}$, (E) CD8/TIL^{high} and CD8/TIL^{low} and (F) CD8/$TIL^{moderate}$ and CD8/TIL^{low}. The relative presentation of trimmed X-SHL8 was compared to that of the maximal response using SHL8, which does not require ERAP1 activity. Data pooled from four independent experimental repeats ±SEM.

Figure 2. ERAP1 allotype combinations from CD8/TIL^{low} tumors have reduced trimming activity.

(A) The total trimming activity for all 20 X-SHL8 substrates for each allotype combination were combined and grouped into CD8/TIL status. Overall trimming for each CD8/TIL group is represented as area under curve (AUC). (B) Table showing both the individual AUC for allotype pairs in each CD8/TIL group as well as the mean for each group. (C) Specificity of ERAP1 trimming activity from those found exclusively in CD8/TIL^{high}, CD8/$TIL^{moderate}$ or CD8/TIL^{low} tumors towards X-SHL8 amino acids grouped based on physicochemical properties; basic, acidic, polar uncharged, aliphatic, aromatic and special. Data from (A-C) pooled from four independent experimental repeats ±SEM (***p = <0.001; **p = <0.01; *p = <0.05).

Figure 3. Presence of anti-HPV E6/E7 epitope $CD8^+$ T cell responses in HPV^+ OPSCC tumors.

Tumors from HPV^+ OPSCC patients were assessed for the presence of $CD8^+$ T cell responses to the HLA-A*0201 restricted HPV E6/E7 epitopes, LLMGTLGIV (LV9), TIHDIILECV (TV10), and KLPQLCTEL (KL9) using dextramers. (A) A representative dot plot showing the presence of all three reactivities in a tumor. (B) Quantification of responses to all three epitopes (LV9, TV10 and KL9) from five HPV^+ OPSCC tumors.

Figure 4. Amino acid specificity of ERAP1 allotype combinations generating the HPV $E7_{82\text{-}90}$ epitope.

E1KO 293T cells were transfected with ERAP1 allotype combinations found in $CD8/TIL^{high}$, $CD8/TIL^{moderate}$ and $CD8/TIL^{low}$ tumors, together with X-LV9 minigenes representing 15 amino acids and assessed for generation of LV9 by BE7A2Z activation. The relative presentation of trimmed X-LV9 was compared to that of the maximal response using LV9, which does not require ERAP1 activity. (A) Heat map representation of % maximal LV9 response towards each amino acid from each allotype combination. Blue represents poor trimming and red represents efficient trimming activity. (B) Total trimming activity of all 15 X-LV9 substrates from each ERAP1 allotype combination grouped into CD8/TIL status and represented as area under curve (AUC). (C) Specificity of ERAP1 trimming activity from those found exclusively in $CD8/TIL^{high}$, $CD8/TIL^{moderate}$ or $CD8/TIL^{low}$ tumors towards X-LV9 amino acids grouped based on physicochemical properties; basic, acidic, polar uncharged, aliphatic, aromatic and special. Data pooled from five independent experimental repeats ±SEM (****p = <0.0001; **p = <0.01; *p = <0.05).

Figure 5. Generation of HPV $E7_{82-90}$ from natural precursors is impaired in CD8/TIL^{low} ERAP1 allotype combinations.

E1KO 293T cells were transfected with ERAP1 allotype combinations from CD8/TIL^{high}, CD8/$TIL^{moderate}$ and CD8/TIL^{low} or the non-functional active site mutant, E320A, together with minigenes encoding final LV9 or extended precursors D-LV9 or ED-LV9 and assessed for trimming activity by the activation of BE7A2Z. (A). Representative line graphs showing the trimming activity of selected ERAP1 allotype combinations from the three CD8/TIL groups. (B and C) The relative maximum LV9 response of ERAP1 allotype combinations from each group, where each symbol represents an individual ERAP1 allotype combination transfection. (B) Trimming activity towards a single amino acid extension (D-LV9) and (C) a double amino acid extension (ED-LV9; **** p = <0.0001; ** p = <0.01). (D and E) The relative maximum LV9 response of each individual ERAP1 allotype combination from CD8/TIL^{high} (black), CD8/$TIL^{moderate}$ (grey), and CD8/TIL^{low} (white) towards D-LV9 (D) and ED-LV9 (E). Data pooled from three independent experimental repeats ±SEM.

Author Manuscript Published OnlineFirst on May 31, 2019; DOI: 10.1158/2326-6066.CIR-18-0498
Author manuscripts have been peer reviewed and accepted for publication but have not yet been edited.

Figure 1

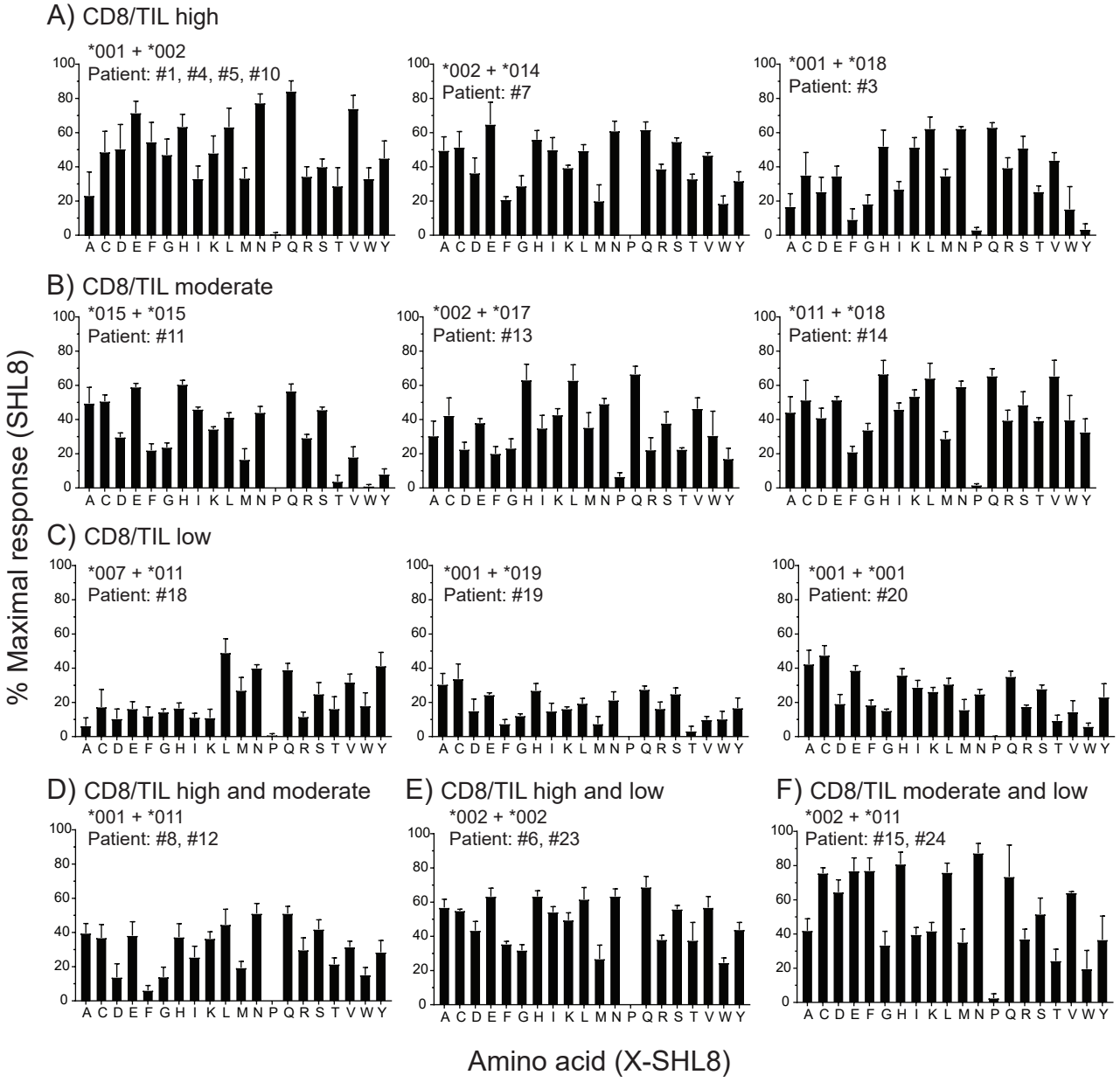

Author Manuscript Published OnlineFirst on May 31, 2019; DOI: 10.1158/2326-6066.CIR-18-0498
Author manuscripts have been peer reviewed and accepted for publication but have not yet been edited.

Figure 2:

A)

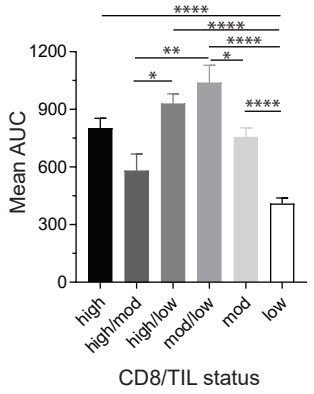

B)

Allotype combination	CD8/TIL status	Overall SHL8 generation (AUC)	Mean AUC
*002+*014	High	812.1	813
*001+*002	"	954.8	
*001+*018	"	672.1	
*001+*011	High + Mod	581.9	581.9
*002+*002	High + Low	930.3	930.3
*002+*011	Mod + Low	1039.1	1039.1
*002+*017	Mod	714.3	748.8
*011+*018	"	892.5	
*015+*015	"	639.6	
*007+*011	Low	415.3	410.0
*001+*019	"	338.1	
*001+*001	"	476.5	

C)

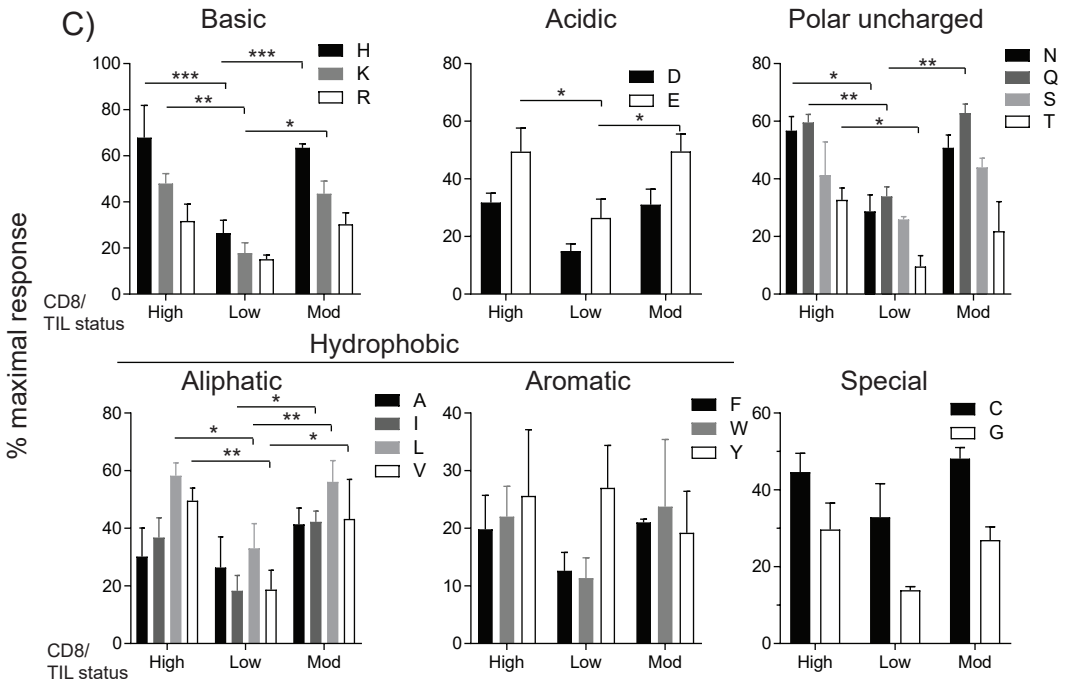

Author Manuscript Published OnlineFirst on May 31, 2019; DOI: 10.1158/2326-6066.CIR-18-0498
Author manuscripts have been peer reviewed and accepted for publication but have not yet been edited.

Figure 3:

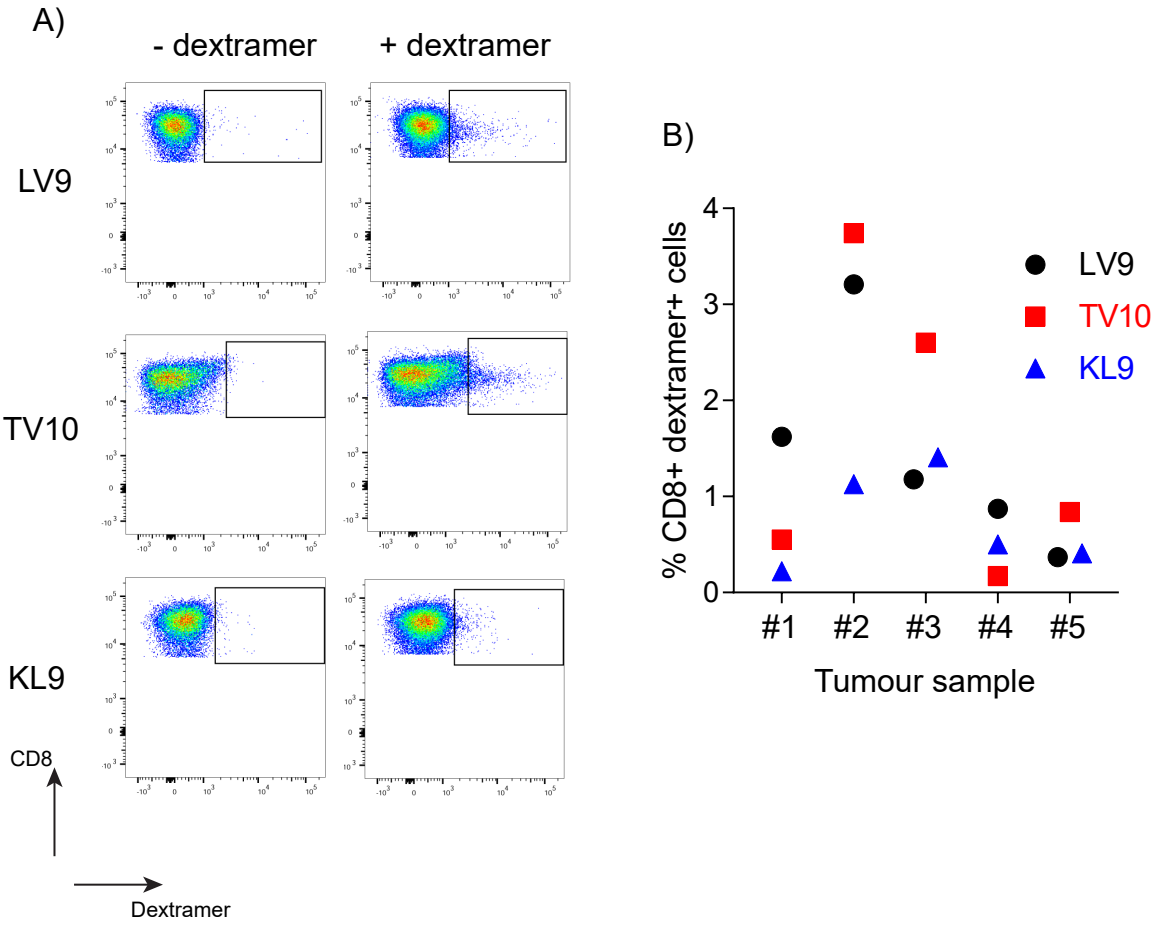

Author Manuscript Published OnlineFirst on May 31, 2019; DOI: 10.1158/2326-6066.CIR-18-0498
Author manuscripts have been peer reviewed and accepted for publication but have not yet been edited.

Figure 4:

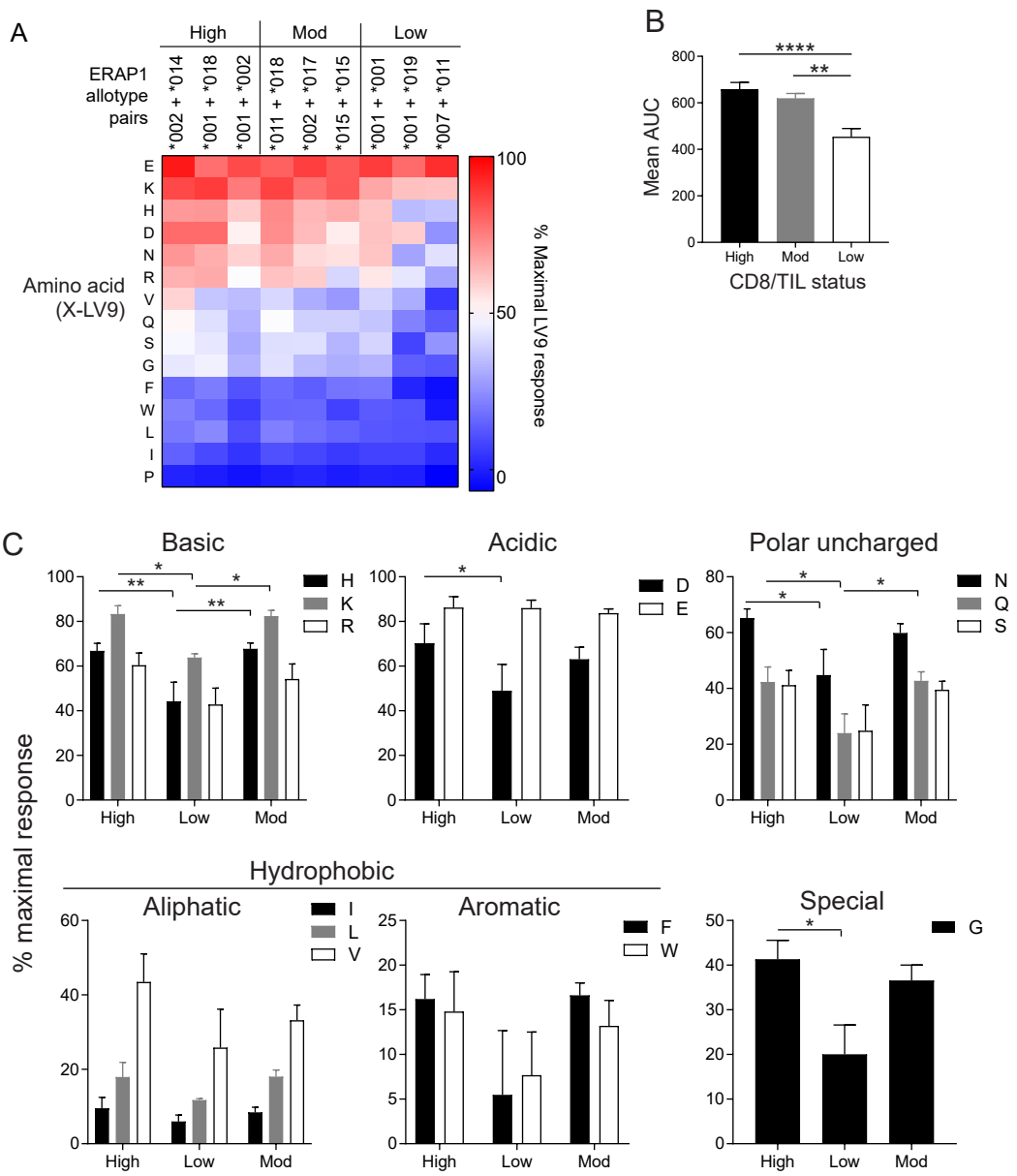

Author Manuscript Published OnlineFirst on May 31, 2019; DOI: 10.1158/2326-6066.CIR-18-0498
Author manuscripts have been peer reviewed and accepted for publication but have not yet been edited.

Figure 5:

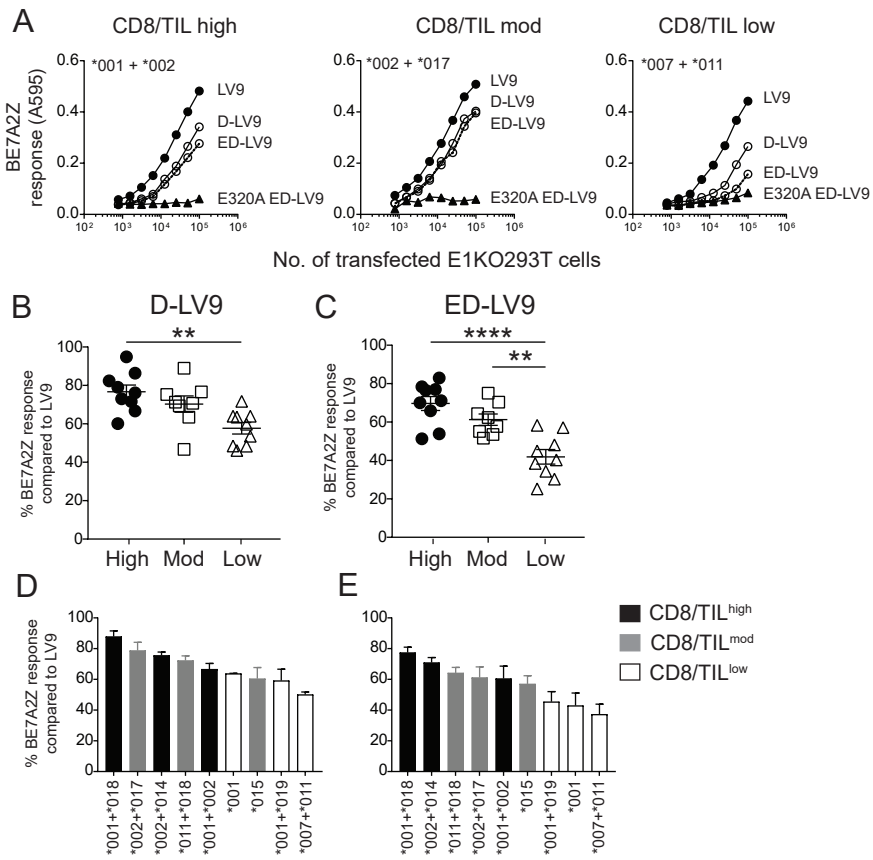

AACR American Association for Cancer Research

Cancer Immunology Research

HPV epitope processing differences correlate with ERAP1 allotype and extent of CD8+ T cell tumor infiltration in OPSCC

Emma Reeves, Oliver Wood, Christian H Ottensmeier, et al.

Cancer Immunol Res Published OnlineFirst May 31, 2019.